DOI: 10.1534/genetics.107.073791

Mutational Interference and the Progression of Muller's Ratchet When Mutations Have a Broad Range of Deleterious Effects

R. Jonas Söderberg and Otto G. Berg[1]

Department of Molecular Evolution, The Evolutionary Biology Centre, University of Uppsala, SE-75236 Uppsala, Sweden

Manuscript received March 23, 2007
Accepted for publication August 6, 2007

ABSTRACT

Deleterious mutations can accumulate in asexual haploid genomes through the process known as Muller's ratchet. This process has been described in the literature mostly for the case where all mutations are assumed to have the same effect on fitness. In the more realistic situation, deleterious mutations will affect fitness with a wide range of effects, from almost neutral to lethal. To elucidate the behavior of the ratchet in this more realistic case, simulations were carried out in a number of models, one where all mutations have the same effect on selection [one-dimensional (1D) model], one where the deleterious mutations can be divided into two groups with different selective effects [two-dimensional (2D) model], and finally one where the deleterious effects are distributed. The behavior of these models suggests that deleterious mutations can be classified into three different categories, such that the behavior of each can be described in a straightforward way. This makes it possible to predict the ratchet rate for an arbitrary distribution of fitness effects using the results for the well-studied 1D model with a single selection coefficient. The description was tested and shown to work well in simulations where selection coefficients are derived from an exponential distribution.

POPULATIONS that reproduce asexually can accumulate deleterious mutations in a process now known as Muller's ratchet (Muller 1964; Felsenstein 1974). When the genomes in the population do not recombine, different mutations that by chance appear in the same genome will remain linked. If back mutations are rare, this linkage will not be disrupted and all mutations segregating together will influence each other. Although selection will hold back the accumulation of deleterious mutations, when by chance in a finite population all mutation-free individuals have been lost they can not be recreated; this is one irreversible "click" of the ratchet. Now the least loaded class carries one mutation and this class can be lost in the same way, leading to further clicks. The irreversibility of the ratchet can lead to a relentless accumulation of deleterious mutations and possibly to the eventual doom of the species. Another effect of the linkage is that the counterselection on deleterious mutations is considerably weakened. This is often expressed as a reduction in effective population size and leads to a much faster fixation of deleterious mutations than in a corresponding population of recombining genomes (Charlesworth and Charlesworth 1997). These are the two main properties of Muller's ratchet: the irreversibility and the reduction of effective selection.

[1]*Corresponding author:* Department of Molecular Evolution, EBC, Norbyvagen 18C, SE-75236 Uppsala, Sweden. E-mail: otto.berg@ebc.uu.se

Escaping the ratchet has been discussed as one major advantage of sex and recombination (Felsenstein 1974; Maynard Smith 1978; Hurst and Peck 1996; Barton and Charlesworth 1998; Gessler and Xu 1999; Keightly and Eyre-Walker 2000). Furthermore, the degeneration and reduction of the genomes of intracellular symbionts and parasites (Moran 1996; Rispe and Moran 2000; Pettersson and Berg 2007) as well as organelles (Lynch 1996; Bergstrom and Pritchard 1998; Lynch and Blanchard 1998; Loewe 2006) have been suggested as consequences of the ratchet. Interestingly, the recent calculations by Loewe (2006) suggest that the human mitochondrial line could have been under serious threat of extinction from the effects of Muller's ratchet. Also the degeneration of the Y chromosome through lack of recombination has been analyzed as an example of Muller's ratchet (Rice 1994; Gordo and Charlesworth 2000a, 2001). Thus, the properties of the ratchet are of fundamental biological relevance and have received considerable attention in the literature.

Deleterious mutations can accumulate also in populations that are of such small size that purifying selection becomes inefficient. However, in such small populations, mutations will become fixed (or lost) relatively fast in comparison to their rate of appearance, and different kinds of mutations will not segregate simultaneously in the population. Thus in this limit, mutations will spread and become fixed independently, and Muller's ratchet will not be effective (Gordo and Charlesworth

2001). At the other extreme, for sufficiently large populations, one can expect that rare beneficial mutations, back mutations, or compensatory mutations will interfere and effectively stop the ratchet. Thus, the ratchet will operate only in certain windows in parameter space.

As a consequence of the strong linkage, deleterious mutations will not segregate independently in the population. The consequent mutational interference is expressed in the rate of the ratchet moving faster than expected from fixations of mutations without linkage. There have been a number of models and calculations presented in the literature describing the rate of Muller's ratchet. Some are based primarily on numerical simulations (Haigh 1978), and others also give closed expressions based on the diffusion approximation (Stephan *et al.* 1993; Gordo and Charlesworth 2000a,b; Stephan and Kim 2002). These calculations consider all mutations as having the same strength of deleterious effect. One particularly obvious case of interference between mutations of different effect is that of background selection (Charlesworth 1994; Stephan *et al.* 1999; Gordo and Charlesworth 2001), where deleterious mutations that are present in the population, but too strongly counterselected to accumulate, increase the accumulation rate of more weakly counterselected ones. In this limit, the effect of the strongly deleterious mutations on the weaker ones can be expressed through a reduced effective population size (Charlesworth 1994; Stephan *et al.* 1999; Gordo and Charlesworth 2001). This size is given by the number of individuals that do not carry any strongly deleterious mutations, as only these individuals will contribute descendants in the long run. The interference between deleterious mutations of two different, but similar, strengths can be described by a weighted average (Gordo and Charlesworth 2001). Some simulations consider deleterious mutations with a distribution of selective effects (Butcher 1995; Gessler and Xu 1999). However, there are no analytical expressions available that predict the rate of the ratchet in this general case and it is our purpose here to fill that gap.

In this communication we study in more detail the effects on the ratchet from deleterious mutations of different effects. The main focus is to define the parameter values where the ratchet operates and to explore how these values are influenced by the mutational interference. There are two main aspects of the ratchet that are of interest here: the rate of mutation fixation and the rate of fitness loss. Most of the calculations are based on the model by Haigh (1978), suitably extended to account for mutations with different deleterious effects. After first describing the models, we briefly consider the original Haigh model [one-dimensional (1D)] and present the results in a somewhat new light that emphasizes some invariant properties of this model. Then we study in more detail an extended Haigh model with two groups of mutations [two-dimensional (2D) model] with different selective effects and show how linkage influences the mutation accumulation in the two groups. This expands previous calculations (Gordo and Charlesworth 2001) by considering in more detail a whole range of fitness effects in the two groups from similar to very different. Finally, we consider the more realistic model where the effects of deleterious mutations are distributed over a wide range. On the basis of the results from the 1D and 2D models, we show how mutations with different deleterious effects can be classified into different categories such that the accumulation of mutations in each category can be described in a straightforward way. Through this decomposition, the overall rate of fitness loss in the general case can be estimated directly from the behavior of the 1D ratchet. This description was tested and shown to work well in simulations using an exponential distribution of deleterious effects. Finally, we discuss some applications where a distribution of s-values could have a significant effect on the fitness decline due to Muller's ratchet.

MODELS

We consider a haploid species reproducing asexually with no recombination between genomes. One natural choice of base line for the results is the standard expression for the rate of independent mutation fixation in freely recombining haploid genomes

$$R_{\mathrm{I}} = \frac{2UNs}{e^{2Ns} - 1} \tag{1}$$

(Kimura 1962, 1964). U is the mutation rate and $-s$ ($s > 0$) is the selection coefficient. N is the effective population size, *i.e.*, the size of the Wright–Fisher population used to describe the species. When the "real" population size (N_{real}) is different from N, new mutations enter the population at a rate UN_{real} and the fixation probability for each is $(N/N_{\mathrm{real}})2s/[\exp(2Ns) - 1]$ (Kimura 1964). Thus, Equation 1 holds for the effective population size, N, regardless of whether or not N is equal to N_{real}. Equation 1 refers to the rate of fixation of a particular mutation, but the result is the same if we consider a group of mutations with the same selection coefficient and U being the sum of their corresponding mutation rates. This expression obviously scales with N such that $R_{\mathrm{I}}N$ depends only on the parameter combinations UN and sN, while R_{I}/U depends only on sN.

Haigh's model and its extensions: In its original form, Haigh's model (Haigh 1978) describes the behavior of Muller's ratchet in a population where all mutations occur independently and have equal and independent effects on survival. The idea of the model is to divide a population **X**, consisting of N individuals, into classes based on the number of mutations, k, each individual carries. The expected number in each class is $E(X_k(t+1) \mid \mathbf{X}(t)) = Np_k(t)$. Since the fitness in class k is

$(1 - s)^k$, the distribution of the population follows the expression

$$p_k(t) = \sum_{j=0}^{k} X_{k-j}(t)(1 - s)^{k-j} e^{-U} \frac{U^j}{j!} \Big/ T(t), \qquad (2)$$

where T is the total fitness of the entire population. In each generation a new population was generated by sampling N individuals with replacement according to this distribution. This corresponds a multinomial sampling with parameters N and $\{p_k\}$. Through this sampling, selection acts on the parent population and new mutations are added to the progeny. Equation 2 gives the stationary distribution where the expected number of individuals in each class k is determined by

$$n_k = Ne^{-U/s} \left(\frac{U}{s}\right)^k \Big/ k! \quad (k = 0, 1, 2, \dots). \qquad (3)$$

Without stochastic variations, this would be the distribution of **X**. However, fluctuations in the number of individuals in each class make it possible for n_0 to reach zero at some point. This means that the fittest class has gone extinct. The new best class will then be $k = 1$, shifting the entire equilibrium one step. This is commonly referred to as a "click of the ratchet." We refer to this model with only one kind of mutation (one s-value) as the 1D model.

Different mutations will in general have different selective effects. To account for this, it is convenient to first expand the one-dimensional model to two dimensions. This implies that there are two kinds of mutations with parameters (U_1, s_1 and U_2, s_2), which occur independently in the population. The probability of obtaining several mutations in the same genome in a single time step is diminutive, at least when $U < 1$. This means that the distribution of a class is negligibly affected by individuals with more than one or a few mutations less in the previous time step. This makes computations feasible by allowing a cutoff that reduces the sums over both dimensions. Using this simplifying fact, two different ratchets in the same population give the following two-dimensional distribution of the classes $\mathbf{X}(t + 1)$ in analogy to Equation 2:

$$p_{k,l}(t) = \sum_{j=k-c}^{k} \sum_{i=l-c}^{l} X_{k-j,l-i}(t)(1 - s_1)^{k-j} e^{-U_1} \frac{U_1^j}{j!} (1 - s_2)^{l-i} \times e^{-U_2} \frac{U_2^i}{i!} / T(t). \qquad (4)$$

Here, k and l are the number of mutations of each type, i and j are the indexes of the contributing classes, c is the cutoff (usually four), s and U are the selection coefficient and the mutational rate for the different mutations indexed by the identifier of that specific mutation, and T is the total fitness of the entire system. This model with two groups of mutations is referred to as the 2D model. A similar two-class model—although not based on Haigh's description—has been considered before (Gordo and Charlesworth 2001).

Like the 1D model, the 2D model is implemented as a stochastic generation of a new population in each generation. The initial state is a population where all N individuals contain zero mutations. Equation 4 gives the probabilities for an individual to carry exactly k and l mutations of each kind in the next generation. A sample of N individuals is drawn in proportion to this distribution to obtain the population in the next generation. One click of the ratchet occurs when the number of individuals in the best class of either mutation group becomes zero and a new best class is established with k or l increased by one. To get reliable data we used at least 500 clicks and at least 50,000 generations (whichever occurred last) for each data point. When using a one-dimensional model we used 10 times those numbers; this gave a standard error of at most 1.5% in the estimated click times in 1D and at most 5% in 2D. With so many events included, initial annealing of the population was not deemed necessary. Standard errors were estimated from the distribution of the individual click times for each run. Double precision was used for all variables in the calculations.

Individual-based model: The Haigh model is computationally very efficient as it deals with classes of mutants and not individuals. However, when there are more than two kinds of mutational effects possible, with different U, the classes become too many for the model to handle efficiently. Therefore, in such cases we used a model where all individuals were treated separately. Each individual started with zero mutations of each kind. In each time step a random individual was drawn from the population in proportion to its fitness relative to that of all others and allowed to replicate. Using the different U:s, Poisson-distributed mutations from each class were added to the newborn. To keep the population constant, the new individual replaces another one, chosen completely at random. Since this approach uses overlapping generations, it is assumed that one generation has elapsed after N divisions. Thus, this is a Moran model whose behavior with population N corresponds to a Wright–Fisher model with effective population size $N/2$ (Moran 1958; Waterson 1975; Ewens 1979). This means that all calculations based on the Moran model were carried out with $2N$ individuals for comparison with a standard Wright–Fisher model (or the Haigh model) of population size N. For comparison, we also considered a Wright–Fisher model (nonoverlapping generations) where N individuals were chosen (with replacement) in proportion to their fitness to make up each new generation. New mutations were added to each new individual as described above. We tested these models in the 1D case and found no significant difference between them (Table 1); in all cases tested, the

TABLE 1

Comparison between different simulation models in 1D with $U = 0.05$

s	R/U^a Moran	SD^a Moran	R/U^b WF	SD^b WF	R/U^c Haigh
0.0001	0.936	0.009	0.950	0.006	0.960
0.0002	0.917	0.027	0.897	0.008	0.907
0.0004	0.830	0.022	0.844	0.012	0.854
0.0008	0.751	0.021	0.744	0.008	0.762
0.0016	0.646	0.018	0.648	0.020	0.658
0.0032	0.515	0.010	0.507	0.016	0.520
0.0064	0.354	0.014	0.344	0.008	0.366
0.0128	0.191	0.004	0.187	0.008	0.200
0.0256	0.049	0.001	0.045	0.001	0.050

[a] Moran model run with population size = 1000 for at least 500 clicks and at least 50,000 generations: average and standard deviation from five replicate runs.

[b] Wright–Fisher model run with $N = 500$ for at least 500 clicks and at least 50,000 generations: average and standard deviation from five replicate runs.

[c] Haigh model run with $N = 500$ for at least 5000 clicks and at least 500,000 generations: a single run with estimated standard error of at most 1.5%.

difference between the models is within the statistical error.

Distribution of selective effects: The space of deleterious mutations probably covers a broad range of selective effects. Thus, we considered a generalized model where the selection coefficient for every new mutation that appeared is drawn from an exponential distribution. An individual was chosen for propagation and replacement of a randomly chosen individual, as described for the individual-based model above. A stochastic number of mutations were added to the new individual according to a Poisson distribution with average U. Each new mutation was assigned an s-value drawn from an exponential distribution according to the equation $s = -\bar{s}\ln(\text{rnd})$, where $\bar{s}$ is the average of the distribution and rnd is a random number between 0 and 1; s-values >1 were set to $s = 1$ (lethal). In this case there are no explicit classes of individuals carrying mutations of identical effect, since all mutations have different s-values. Thus, there is no well-defined click rate and the progression of the ratchet can be characterized instead by the average deterioration in fitness over time. Data points were recorded after each 1000 generations and the rate of fitness loss was estimated from the slope of the natural log of the average fitness per individual *vs.* time. Standard errors in these numbers were <5% as estimated from the goodness of the exponential fit. Replicate (two, three, four, or five) runs were carried out and supported this error estimate.

RESULTS

Behavior of the 1D model: The rates of mutation accumulation for various values of U, s, and N have been calculated through stochastic simulation in a number of publications (Haigh 1978; Stephan *et al.* 1993; Charlesworth and Charlesworth 1997; Gordo and Charlesworth 2000a,b). The numerical results of the present calculations based on the Haigh model with a single category of deleterious mutation agree with these previous ones. Some differences with simulations that are not based on the Haigh model (Charlesworth and Charlesworth 1997; Gordo and Charlesworth 2000a,b) can appear in the limit where the ratchet is moving very slowly, but that is of little consequence for the discussion below. Here we present and discuss the results from the 1D Haigh model with a focus on delimiting the parameter region where the ratchet can be effective.

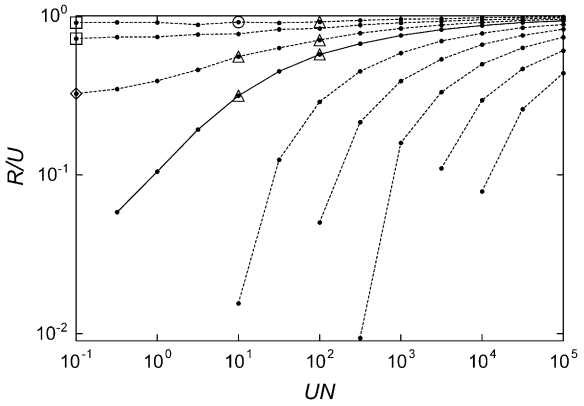

Figure 1.—Normalized ratchet rate R/U *vs.* UN for different values of selection sN in the 1D model: dotted curves from top to bottom, $sN = 0.1$, 0.3, 1, 10, 32, 100, 316, and 10^3; solid curve, $sN = 2.5$. Straight lines are drawn between simulation points. The standard error in the data points is ≤1.5%, *i.e.*, on the order of the size of the solid data points. Some points marked with open symbols were run with several different N-values: squares, $N = 100$, 316, 1000, and 3162; diamond, $N = 100$, 316, and 1000; triangles, $N = 10^2$, 10^3, and 10^4; circle, $N = 10^2$, 10^3, 10^4, and 10^5. The N-values used for the single data points are: $N = 10^3$ for $UN < 3 \times 10^3$, $N = 10^4$ for $3 \times 10^3 < UN < 3 \times 10^4$, and $N = 10^5$ for $UN > 3 \times 10^4$.

Just like the result for independent fixations, Equation 1, the ratchet rate R is found to scale with N such that RN, or R/U, depends only on the parameter combinations UN and sN. This is as expected from diffusion theory (Ewens 1979; McVean and Charlesworth 2000) and, indeed, the analytical approximations given (Stephan *et al.* 1993; Gordo and Charlesworth 2000a,b) show this scaling explicitly. The scaling has recently been used in the description of the ratchet effects for transposable elements (Dolgin and Charlesworth 2006). In our simulations, scaling is found to hold well over a broad range of parameter values. Marked data points in Figure 1 were simulated with N-values varying from 100 to 10^3 or 10^4 and in one case up to 10^5. In all tested cases, scaling holds within the statistical uncertainty of the method of at most 1.5% error in estimated click rates. There could be discrepancies for very small

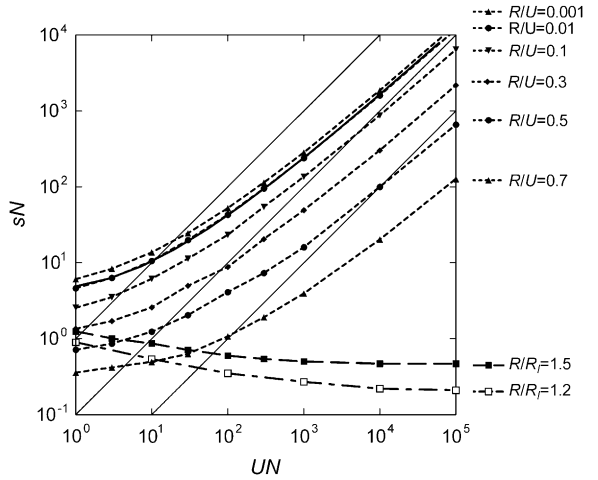

FIGURE 2.—The window of operation as a contour plot showing the values for UN and sN where (dotted curves from bottom to top) $R/U = 0.7$, 0.5, 0.3, 0.1, 0.01, and 0.001. The solid curve is $UN = sN\ln(sN/4)$, which almost exactly overlaps the dotted curve for $R/U = 0.01$. The dashed curve with solid squares is where $R/R_I = 1.5$ and the dashed-dotted curve with open squares is where $R/R_I = 1.2$. Straight lines have been drawn between simulation points. Thin solid lines show changes in N at constant s and U; from top to bottom, $s/U = 1$, 0.1, and 0.01. The N-values used varied as in Figure 1.

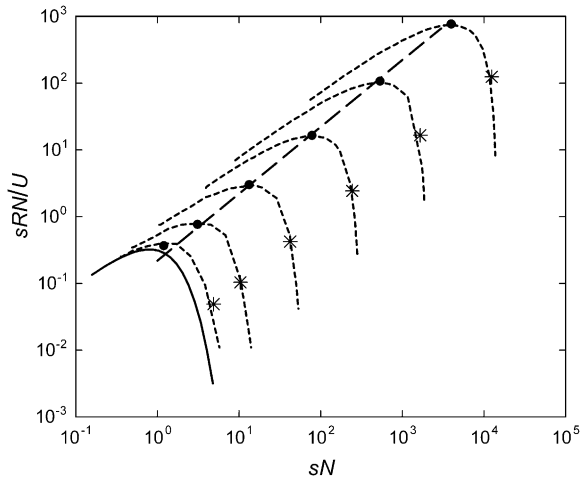

FIGURE 3.—Scaled rate of fitness loss as a function of sN. The dotted curves are for (from left to right) $UN = 1$, 10, 100, 10^3, 10^4, and 10^5. The solid curve shows the same thing for independent fixations (Equation 1); this curve is independent of UN and corresponds to the rate in the limit $UN \ll 1$. The dashed line is $0.22sN$, which approximately follows the empirical maximum points determined by Equation 6. The asterisks show the points where the ratchet is assumed to be stalled according to Equation 5.

N-values, but none were detected above $N = 100$, which was the lower limit we tested. We did not see any systematic departures with increasing N-values. Very large N-values can be too slow to simulate, but the parameter region where the ratchet runs slowly is also where the analytical expressions are expected to hold best (STEPHAN and KIM 2002). As a consequence, to speed up the simulations, properties of a large population can be calculated from those of a smaller one if U and s are increased in proportion (as long as $s < 1$ still holds). Even though the model has three independent parameters (U, s, N), all calculations can be carried out and all results reported in terms of RN (or R/U) as a function of only the two parameters UN and sN.

Figure 1 shows the results of the normalized ratchet rate R/U as a function of UN for various values of sN. This is the ratchet rate relative to neutral fixation. Another possibility would be to consider R/R_I, the ratchet rate relative to independent fixations. However, R/R_I becomes unreasonably large for large values of sN and is not very useful for that reason. The results can be summarized very conveniently and compactly as displayed in Figure 2, which shows a contour plot for different values of R/U *vs.* UN and sN. On the basis of this graph, it is very simple to see how the 1D ratchet will behave for almost any choice of parameter values U, s, and N. As is well known, the maximum click rate is reached in the neutral limit ($s = 0$) where $R = R_I = U$. Near-independent mutation accumulation will occur for small values of s where R approaches R_I. If we arbitrarily choose $R/R_I < 1.5$ as the criterion, then the dashed line in Figure 2 shows the limit below which independent fixation is expected. This corresponds to $sN \sim 1$ in order of magnitude. Using a more stringent criterion, *e.g.*, $R/R_I < 1.2$, lowers this limit somewhat (Figure 2). In Figures 1 and 3, it can be seen that R/U approaches R_I/U when $UN < 1$. Thus, for $UN < 1$ and/or $sN < 1$, deleterious mutations spread largely independently regardless of whether or not recombination takes place, and the ratchet does not operate—or has little effect—in this region of parameter space.

In Figure 2 (solid curve) it can also be seen that $R/U = 0.01$ holds approximately when

$$sN\ln(sN/4) = UN. \tag{5}$$

This empirical relationship predicts the sN-value for which $R/U = 0.01$ to within a few percent in the parameter region $3 \leq UN \leq 10^5$, while the error is ~10% for $UN = 1$. Even if $R/U = 0.01$ could correspond to an appreciable ratchet rate (if U is very large), the ratchet rate decreases very sharply with increasing s and/or decreasing U in this parameter region and quickly reaches vanishingly small values; the contour lines for small values of R/U in Figure 2 bunch up here. A similar relation for stopping the ratchet has been suggested before (GORDO and CHARLESWORTH, 2000a, 2001), but with the numerical factor 15 instead of 4. Clearly, with this higher limit, the ratchet would be even more severely slowed down; however, in this case, there is no simple relationship with R/U. As we shall see below, Equation 5 plays an important role also in describing the interference between deleterious mutations of different effect. Thus, we consider Equation 5, or $s\ln(sN/4) > U$, as the

limit where the ratchet has stopped. This limit corresponds to the case when the stationary estimate of the size of the best class, Equation 3, satisfies $n_0 > 4/s$. Taken together, the ratchet can operate only in the wedge-shaped region of parameter space roughly delimited by the solid and dashed curves in Figure 2; it is only in this region that recombination can work as a significant relief for Muller's ratchet.

Figure 2 is based on the scaling properties where R/U as a function of UN and sN is independent of N. Changes in population size (N), at constant U and s, therefore correspond to movement along a straight line with slope 1 in Figure 2; three such lines are indicated. For example, along the bottom straight line where $s/U = 0.01$, it can be seen that a decrease in R/U from 0.7 to 0.5 would require an increase in N by a factor of ~100. Thus, the ratchet rate depends relatively weakly on N. For $s/U > 10$, the ratchet cannot operate regardless of the population size.

The click rate, R, increases with decreasing s toward the maximum $R = U$ for neutral changes with $s = 0$. It is also interesting to consider the rate of fitness loss, sR. For small s, the mutations are accumulating fast but with small effect, while for large s the ratchet stops (Lynch and Gabriel 1990; Butcher 1995; Loewe 2006). In Figure 3, the scaled rate of fitness loss, sRN/U, is plotted as a function of sN for different values of UN. This scaled rate was chosen such that it depends only on UN and sN. To find the actual rate of fitness loss, sR, for any choice of parameters (U, s, N), one will have to read off the scaled rate for the appropriate UN and sN and then multiply by U/N. In the whole region of parameter space investigated ($1 \leq UN \leq 10^5$), we find that the rate of fitness loss at given UN has a maximum for an s-value, s_m, approximately determined by the empirical relation

$$UN \approx 3 s_m N \ln(s_m N). \quad (6)$$

This expression gives the location of the maximum to within ±5% in the range of UN-values studied. At this maximum, the click rate R satisfies $R/U \approx 0.20$–0.25, see Figure 3. Figure 3 displays another approximate invariance in the results: all curves for sRN/U can be fairly well superimposed on each other if shifted along the dashed line connecting their maxima. For $UN > 10$, the shifted curves are virtually indistinguishable, but for smaller UN the height and shape of the curves are not quite in agreement.

Interference between mutations in the 2D model: For systems containing two kinds of deleterious mutations, ratchets can operate on one, both, or none of the groups. Clearly, due to the linkage, there is a single ratchet operating. However, mutations with different effects will accumulate at different rates, and it is convenient to discuss the behavior as that of two interfering ratchets. Our results on the click rates agree with those of Gordo and Charlesworth (2001), where the parameters overlap. One way to visualize the interference

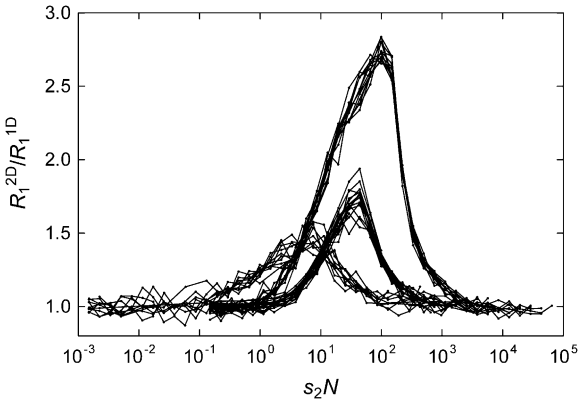

Figure 4.—The ratchet speed for group 1 relative to what it would be by itself without interference, shown as a function of the selection in group 2. The three families shown have parameter values (from highest peak to lowest) (U_1N, s_1N, U_2N) = (100, 10, 500), (100, 10, 100), and (0.5, 0.5, 10). Values of N varied between 100 and 70,000 for the 13–17 different curves in each family. Considering the different curves in each family as replicate runs, the maximum relative standard deviation in each family is ~5%.

in the 2D ratchet is to plot the ratchet speed for one group of mutations *vs.* changes in a parameter for the other group. When doing this, one can clearly see families of curves appearing for sets of different UN and sN (Figure 4). This means that the scaling property for the ratchet speeds holds also for the 2D model. For all ranges of parameters that we have tried (s_1, U_1, s_2, and U_2 were all varied in the range 0.00001–0.9, while N varied between 100 and 70,000), the speeds of the ratchets, multiplied by population size (N), are nearly invariant if N changes while keeping s_1N, U_1N and s_2N, U_2N constant. The erratic behavior of data points for the same N-value, which are connected by lines, shows the extent of stochastic scatter in Figure 4. Overall deviations within each curve family are small and the scaling with N holds well throughout. Thus, the properties of large populations can be inferred from calculations at smaller N if s- and U-values are increased in proportion. This can considerably speed up the calculations, and, like the 1D case, it allows a more compact data presentation by reducing the number of free variables.

Figure 4 shows the increase in the click rate for one group of mutations (with parameters U_1 and s_1) when the selective properties of a second group (with parameters U_2 and s_2) are changed. On the x-axis is the selection coefficient of the second mutation scaled by N. The y-axis shows the ratio of the click rate in the first group relative to that it would have if the second group were not present. Thus, this graph shows the relative influence of the second mutation on the clicking rate of the first. As one can clearly see, interference is present only in a window of parameter values and has a very distinct maximum. The lower limit is fairly obvious: interference disappears for $s_2N < 1$, *i.e.*, when the second

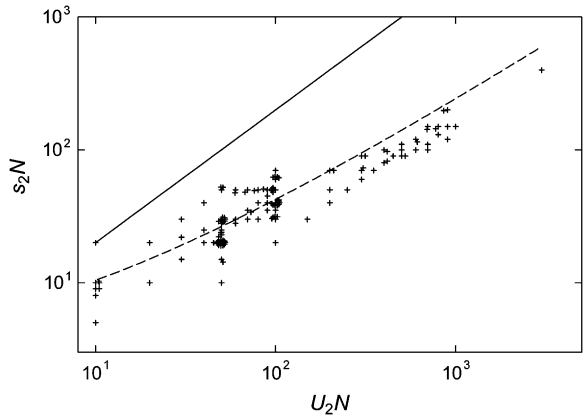

FIGURE 5.—The window of interference and the location of maximum interference. Interference is possible in the region $1 < s_2N < 2U_2N$. The data points are the locations of maximum interference estimated from curves like those in Figure 4. The solid line is the upper limit of interference ($s_2/U_2 = 2$) and the dashed line is the location of the points where group 2 would stop clicking if it were alone, Equation 5.

group approaches neutrality. As can be seen in Figure 4, there can be cases with some interference also from sites with $s_2N < 1$, but this is only when group 1 is also of weak effect ($s_1N < 1$) and the effect on total fitness loss is small. The upper limit is more variable: interference seems to disappear when $s_2N > 2U_2N$. In this limit, not only would mutations in group 2 have stopped accumulating, but also most individuals in the population would be totally free of mutations from this group [$n_0/N = \exp(-U_2/s_2) > \exp(-0.5) = 0.6$; see Equation 3]; mutations in group 2 are simply under too strong counterselection to have a significant presence in the population. Outside the window of interference, mutations in the two groups can be considered as accumulating independently of each other.

The location of maximum interference can be identified as the point where the second group would stop clicking if it were alone. In the 1D model (see Figure 2 and Equation 5), this would occur approximately when $s_2N\exp(-U_2/s_2) = 4$. In Figure 5, we have plotted the location of the maximum points from Figure 4 and from other similar calculations. They follow this relation very well. Some scatter in Figure 5 is due to the difficulty of identifying the precise location of maxima in curves like those of Figure 4; there may also be some scatter due to a small influence from differences in the parameters U_1N and s_1N. It should also be noted that mutations in group 2 will not actually have stopped at these locations; the linkage to group 1 will of course provide some interference and speed up the accumulation in group 2 as well. Nevertheless, the 1D properties provide some very useful guidelines for the interference effects.

While there may be some small influence from the parameters U_1N and s_1N on the location of the maximum interference, these parameters have their largest effect on the amplitude of the maximum. In principle, the largest interference will appear in a group that considered by itself would be stalled or nearly stalled, but where the addition of a second group is sufficient to start the ratchet. Small interference would appear in a group that is nearly neutral and already clicking at a near-maximal rate.

Total rate of fitness loss in the 2D model: The effects of Muller's ratchet on the rate of fitness loss in a population have been discussed mostly in terms of a 1D model where all mutations have the same (or some average) deleterious effect. For discussion and computational convenience it would therefore be useful if the 2D model—or any model where mutations have different effects—could be described in terms of some equivalent 1D model, *e.g.*, by using average values. Due to the linkage, or interference, the total rate of fitness loss in the two groups will of course be faster than if mutations accumulate in each group independently. Outside the window of interference, the total rate of fitness loss could be described as the sum of two independent 1D ratchets. On the other hand, in this region one of the groups is either near neutral or too strongly counterselected to contribute much to the total fitness loss. Two groups that have the same selective effect ($s_1 = s_2 = s$), will behave like a single 1D ratchet with parameters s and $U = U_1 + U_2$. In the region where s_1 is very close to s_2 it is possible to describe the rate of fitness loss as a 1D model with $U = U_1 + U_2$ and an effective s-value that is the harmonic mean of s_1 and s_2: $s = U/(U_1/s_1 + U_2/s_2)$ (GORDO and CHARLESWORTH, 2001). For most parameter combinations it seems that a geometric average using $s = (s_1^{U_1}s_2^{U_2})^{1/U}$ works even better (Figure 6). In the applications below, we use the arithmetic mean, $s = (U_1s_1 + U_2s_2)/U$, which is simpler to work with and gives similar results (Figure 6) when s_1 and s_2 are close. In the limit of background selection (CHARLESWORTH 1994; STEPHAN *et al.* 1999; GORDO and CHARLESWORTH 2001) a group that is stalled or nearly stalled will influence the other group mostly as a decrease in the effective population size. That is, in the parameter region where group 2 has stalled, the system can be well described as a 1D model with $s = s_1$, $U = U_1$, and N replaced by $N\exp(-U_2/s_2)$; see Figure 6.

We looked at other ways of describing the effects of two different mutation classes on the total rate of fitness loss as determined by some average s-value, without finding any method that worked over a broad range of parameter values. Thus, the weighted mean is useful only if the two s-values are very close to each other (no more than a factor 4 apart for the arithmetic mean), while using the effective-population size reduction to describe the background selection works well only when one of the groups is (nearly) stalled (GORDO and CHARLESWORTH 2001). As is seen below, although these two limits appear very restrictive, they can still provide a

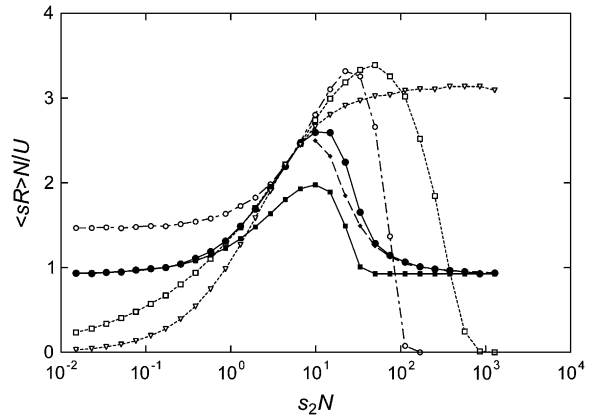

FIGURE 6.—The scaled total rate of fitness loss in a system with two different kinds of mutations when selection in the second group (s_2N) is changed (solid circles), calculated as $(s_1R_1^{2D} + s_2R_2^{2D})N/(U_1 + U_2)$. The solid squares show the ratchet considered as the sum of two independent 1D ratchets calculated as $(s_1R_1^{1D} + s_2R_2^{1D})N/(U_1 + U_2)$. The open symbols show the various approximations: the 1D ratchet with $U = U_1 + U_2$ and arithmetic mean s (open circles, dashed-dotted line); the 1D ratchet with $U = U_1 + U_2$ and harmonic mean s (open triangles, dotted line); the 1D ratchet with $U = U_1 + U_2$ and geometric mean s (open squares, dotted line); and the 1D ratchet with $U = U_1$, $s = s_1$, and effective population size $N\exp(-U_2/s_2)$ (open diamonds, dashed line). Parameter values used: $U_1N = 60$, $s_1N = 5$, $U_2N = 60$. $N = 10^3$ is used in these calculations.

useful basis for the description of the total rate of fitness loss in a system where the deleterious mutations have a general distribution of s-values.

Distribution of selective effects: The calculations with two kinds of selective effects suggest that deleterious mutations with similar s-values can be grouped together in categories. In principle, we can distinguish three major categories through their effect on the ratchet:

1. Sites where mutations are so strongly counterselected that the ratchet clicks extremely slowly or not at all will nevertheless influence the ratchet process in the other two categories through background selection.
2. Sites with intermediate counterselection will accumulate mutations. These are the sites that are most affected by the ratchet.
3. Sites under weak counterselection (near neutral with $sN < 1$) will accumulate mutations at rates approaching the rates for independent fixation. However, they will not affect the ratchet rates in the other categories.

The nonclicking sites in category 1 are expected to carry mutations distributed according to the stationary-state Poisson distribution, Equation 3. The probability that an individual in the population does not carry any mutations in this group is $P_0 = \exp(-\Sigma(u_i/s_i))$. Here, u_i and s_i are the mutation rate and selection for each site (i) and the sum is taken over all sites where s is too large to allow fixation. In the 1D model (single s-value) we saw that the ratchet stops when $sN > 4\exp(U/s)$, Equation 5. With a distribution of s-values, it may be expected that the ratchet is stalled for all mutations where $s_jN > 4\exp(\Sigma(u_i/s_i))$. In this relationship, the sum in the exponent should be taken for all $s_i \geq s_j$, where s_j is the smallest value for which the inequality holds. Then the effective population size would be implicitly defined from

$$N_{eb} = N\exp\left(-\sum_{s_iN_{eb}\geq 4}(u_i/s_i)\right), \qquad (7)$$

where the sum is taken over all sites where $s_iN_{eb} \geq 4$. Through this sum, the right-hand side (RHS) of Equation 7 can be calculated for any choice of N_{eb} and the solution to Equation 7 will be determined by that value for which RHS $= N_{eb}$. While N is the effective size of the Wright–Fisher population with no linkage effects, N_{eb} would be the effective size of the same population when linkage effects are accounted for through background selection. By definition, N_{eb} is the size of the best class in category 1, which will serve as the effective population size for the mutation accumulation in the other two categories due to background selection. There may be slow clicks in this category so that the best class actually could carry a few mutations, but when clicking is slow, the stationary distributions will become established between clicks. Equation 7 is a key relationship as it defines the distinction between categories 1 and 2 as well as the strength of the background selection.

Sites in category 2 will be defined by s-values in the narrow range $1 < s_iN_{eb} < 4$. Since the s-values in this category are fairly close, the sites can be lumped together in a single group with a single s-value as the weighted average $s_2 = \Sigma u_is_i/\Sigma u_i$ and total mutation rate $U_2 = \Sigma u_i$. Thus, mutations in category 2 can be treated approximately as a 1D ratchet with parameters s_2, U_2, and N_{eb}. Although this category is defined from its s-values where the ratchet can be expected to operate, it is possible that $U_2N_{eb} < 1$ so that independent fixations will dominate also in this category. Effective population sizes calculated from neutral diversity would include the background selection from all stalled or nearly stalled sites (category 1) in the ratchet (CHARLESWORTH *et al.* 1993), but also sites in category 2 that are actually clicking could contribute; this effect is more difficult to estimate.

Sites in category 3 are defined by having such low s-values that they accumulate mutations without much influence on the mutation accumulation in the other groups: $s_iN_{eb} < 1$. Note that these mutations may accumulate like near-neutral ones with a rate approaching the mutation rate, but could still contribute to an appreciable fitness loss, particularly if N_{eb} is small. Mutations in this category will accumulate and eventually reach a mutation–selection–drift balance where back mutations interfere. Although by themselves not part of the ratchet, mutation fixation at sites in category 3 could

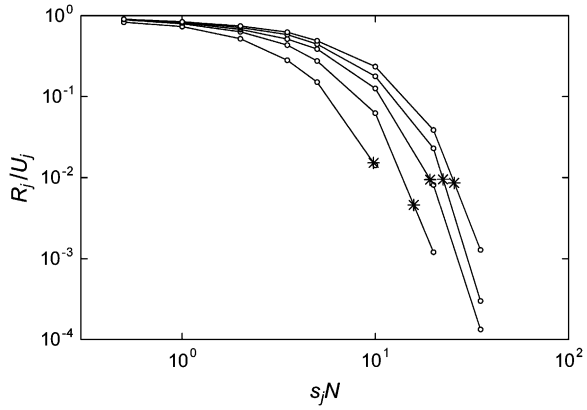

FIGURE 7.—The clicking rate in 10 different groups of deleterious mutations normalized to the mutation rate in each group. The selection in each group is shown on the *x*-axis. The same U_j-value ($U_j = U/10$ for $j = 1, 2, \ldots, 10$) was used in all groups and five different sets were run with (from top to bottom line) $UN = 250$, 200, 150, 100, and 50. Simulations in this case are based on the Moran model, and as described in the MODEL section, this is implemented by running the simulations with the population size $2N$ for any given N-value; $N = 500$ is used here. The asterisks indicate the point below which the mutations are considered stalled according to Equation 8.

be influenced through background selection by the ratchet effects in the other two categories (MCVEAN and CHARLESWORTH 1999, 2000).

To test the grouping of mutation categories with different effects we studied a generalized model with 10 groups as described in the MODEL section. Figure 7 shows the speed of the ratchet for each group in a 10-group system. For simplicity, $U_j = U/10$ (for $j = 1, \ldots, 10$) was taken to be the same for each group and five different genomic U-values were tested (the five curves in Figure 7). The data points correspond to the ratchet rate for each mutation group with Ns_j indicated along the *x*-axis. The groups below the asterisks in Figure 7 are expected to be stalled according to the criterion discussed above:

$$s_jN > 4\exp\left(\sum_{k=j}^{10}(U_k/s_k)\right). \tag{8}$$

There is a very good agreement between the expectation from Equation 8 and the observations in the extended 10-group model. An exact agreement cannot be expected, mostly because interference from category 2 will effectively decrease the size of the least-loaded class in category 1 and thereby increase the value of s for which the ratchet stops.

Exponential distribution of *s*-values: Below we consider a population of organisms with an effective population size N_{eb} and genomic deleterious mutation rate U. It is assumed that the deleterious effects have an exponential distribution for $0 < s < 1$ with average $\bar{s}$ such that the density of s-values is given by

$$\rho(s) = \frac{1}{\bar{s}(1 - e^{-1/\bar{s}})}\, e^{-s/\bar{s}} \approx \frac{1}{\bar{s}} e^{-s/\bar{s}}. \tag{9}$$

To this one could add strictly neutral ($s = 0$) as well as lethal ($s = 1$) mutations, which may form distinct groups but do not affect the ratchet. The approximation holds if $\bar{s} \ll 1$, which is most often the case and is assumed below for simplicity. Without much loss of generality, it is further assumed that all mutations have the same rate. Then the mutation rates in each category can be calculated as appropriate averages over the distribution

$$\begin{aligned} U_1 &= U\int_{4/N_{eb}}^{1} \rho(s)\,ds = Ue^{-4/\bar{s}N_{eb}} \\ U_2 &= U\int_{1/N_{eb}}^{4/N_{eb}} \rho(s)\,ds = U\left(e^{-1/\bar{s}N_{eb}} - e^{-4/\bar{s}N_{eb}}\right) \\ U_3 &= U\int_{0}^{1/N_{eb}} \rho(s)\,ds = U\left(1 - e^{-1/\bar{s}N_{eb}}\right). \end{aligned} \tag{10}$$

Similarly, the average s-value in category 2 is found to be

$$\begin{aligned} s_2 &= \frac{\int_{1/N_{eb}}^{4/N_{eb}} s\rho(s)\,ds}{\int_{1/N_{eb}}^{4/N_{eb}} \rho(s)\,ds} \\ &= \frac{(1 + \bar{s}N_{eb})e^{-1/\bar{s}N_{eb}} - (4 + \bar{s}N_{eb})e^{-4/\bar{s}N_{eb}}}{N_{eb}\left(e^{-1/\bar{s}N_{eb}} - e^{-4/\bar{s}N_{eb}}\right)}. \end{aligned} \tag{11}$$

In these expressions, N_{eb} is defined from the stalled sites in category 1, Equation 7. With the exponential distribution, this can be expressed as

$$\begin{aligned} \frac{N_{eb}}{N} &= \exp\left(-\frac{U}{\bar{s}}\int_{4/N_{eb}\bar{s}}^{1/\bar{s}} \frac{1}{x}e^{-x}\,dx\right) \\ &\approx \left(\frac{7.12}{N_{eb}\bar{s}}\right)^{U/\bar{s}} \exp\left(-\frac{4U}{N_{eb}\bar{s}^2}\right), \end{aligned} \tag{12}$$

where N would be the effective size of the same population without linkage and background selection. The approximation is valid for $\bar{s}N_{eb} \gg 4$ when the exponential integral in the exponent can be approximated with the first terms of a series expansion. Only when $N_{eb}/N \ll 1$ will there be a significant influence on the mutation accumulation from the stalled sites.

To estimate the overall rate of fitness loss we can estimate and sum the rates in categories 2 and 3: $\langle sR\rangle = \langle sR\rangle_2 + \langle sR\rangle_3$. For the approximately independent fixations in category 3 ($0 < sN_{eb} < 1$), the rate of fitness loss can be calculated as the integral over the rate given by Equation 1:

$$\langle sR\rangle_3 = \int_0^{1/N_{eb}} \rho(s)\frac{2UN_{eb}s^2}{e^{2N_{eb}s} - 1}\,ds \approx \frac{U}{4\bar{s}N_{eb}^2}. \tag{13}$$

The approximation holds very well in the limit $\bar{s}N_e \gg 1$. The sites in category 2 will behave approximately as a 1D ratchet with parameters s_2, U_2, and N_{eb}, determined by Equations 10–12. Thus $\langle sR\rangle_2 \approx s_2R_2^{1D}$, where R_2^{1D} in

TABLE 2

Average rate of fitness loss with an exponential distribution of *s*-values

N^a	UN	$\bar{s}N$	Repl[b]	$\langle sR\rangle^c$ ($\times 10^6$)	$N_{eb}{}^d$	$U_2N_{eb}{}^e$	$s_2N_{eb}{}^f$	$\langle sR\rangle_2{}^g$ ($\times 10^6$)	$\langle sR\rangle_3{}^h$ ($\times 10^6$)
500	3	10	3	1.5 (0.04)	419	0.671	2.41	0.84	0.39
500	10	0.1	2	3.4 (0.05)	500	4.5×10^{-4}	1.10	~0	3.3
500	10	1	2	15 (0.001)	484	3.29	1.83	7.4 (5.6)	5.9
500	10	10	2	12 (0.5)	323	2.06	2.38	8.0 (8.1)	2.2
500	10	30	2	3.2 (0.03)	333	0.883	2.46	2.0	0.72
500	10	100	4	0.49 (0.03)	391	0.289	2.49	0.26	0.16
500	25	5	3	72 (1.1)	283	6.50	2.24	54 (52)	13
500	100	1	3	220 (0.5)	425	25.5	1.76	120 (110)	71
500	100	10	2	630 (5)	147	13.4	2.25	530 (500)	94
500	100	100	5	120 (4)	124	2.71	2.47	80 (88)	16
5000	1000	10	2	160 (2)	740	65.4	2.03	140 (130)	31
5000	1000	100	2	310 (6)	245	18.3	2.35	280 (280)	36
5000	1000	1000	4	12 (0.2)	412	2.91	2.49	8.2 (8.8)	1.4
5000	1000	10		(As above)	898[i]	90[i]	2.33[i]	150[i]	22[i]
5000	1000	100		(As above)	294[i]	24.4[i]	2.79[i]	310[i]	26[i]
5000	1000	1000		(As above)	456[i]	38.3[i]	3.00[i]	9.0[i]	1.2[i]

[a] Population size of the corresponding Wright–Fisher model.
[b] Number of replicate runs.
[c] Rate of fitness loss calculated from the simulation using the exponentially distributed *s*-values in a Moran model with population size $2N$: in parentheses, the standard deviation in the replicate runs is shown. Runs were between 10^4 and 2.14×10^6 generations; for each parameter combination, at least one run was longer than 2×10^5 generations.
[d] Effective population size calculated from the integral in Equation 12.
[e] Effective mutation rate in category 2 from Equation 10.
[f] Effective selection coefficient in category 2 from Equation 11.
[g] Rate of fitness loss in category 2 calculated as $s_2R_2^{1D}$ from a 1D simulation with parameters N_{eb}, U_2, and s_2 (within parentheses, calculation using Equation 14).
[h] Rate of fitness loss in category 3 calculated from the integral in Equation 13.
[i] Predicted results when the border to category 1 is at $sN_{eb} > 5$.

general can be calculated from 1D simulations or from analytical approximations (Stephan *et al.* 1993; Gordo and Charlesworth 2000a,b; Stephan and Kim 2002). In the limit $\bar{s}N_{eb} \gg 4$, Equation 11 gives $s_2N_{eb} \approx 2.5$ and the calculations can be simplified further. In this limit, the 1D ratchet will click with a relative rate that can be approximated by the empirical relation $R_2/U_2 \approx 0.1[\ln(U_2N_{eb}) + 1]$ within $\pm 10\%$ when $1 \le U_2N_{eb} \le 3000$ (*cf.* Figure 1). Thus, in these limits

$$\langle sR\rangle_2 \approx s_2R_2 \approx 0.1[\ln(U_2N_{eb}) + 1]U_2s_2. \qquad (14)$$

Furthermore, in the limit $\bar{s}N_{eb} \gg 4$, one finds $U_2N_{eb} \approx 3U/\bar{s}$ from Equation 10. In this limit the total rate of fitness loss will be

$$\langle sR\rangle = \langle sR\rangle_2 + \langle sR\rangle_3 \approx \left[\frac{3}{4}\ln(3U/\bar{s}) + 1\right]\frac{U}{\bar{s}N_{eb}^2}. \qquad (15)$$

Thus, with an exponential distribution of *s*-values and the limits $\bar{s}N_{eb} \gg 4$ and $0.3 < U/\bar{s} < 1000$, the fitness loss rate can be expressed very simply as in Equation 15. Linkage effects can be very strong through the background selection as expressed by N_{eb} in Equation 12.

We have tested this description against simulations where deleterious mutations were drawn from an exponential distribution of *s*-values and the results are shown in Table 2 and Figure 8. The average rate of fitness loss was estimated from the slope of the natural log of the average fitness per individual *vs.* time. In all cases tested, the simulated results agree with the estimated fitness loss rate calculated from the three categories defined here; the discrepancy is <20% and in most cases much smaller. The fitness loss in category 2 was calculated from a 1D simulation using values of N_{eb}, U_2, and s_2 calculated from the full Equations 10–12 and the fitness loss in category 3 was calculated from the integral in Equation 13. In the appropriate limits, also Equation 14 and Equation 15 hold very well. The general effect of the distributed *s*-values, compared to the 1D case with $s = \bar{s}$ for all deleterious mutations, is to considerably speed up the ratchet where it is slow or even stopped and to slow it down somewhat in parameter regions where the 1D ratchet would be moving fast (Figure 8). The main effect is to blur the very sharp limit where the 1D ratchet stops functioning (Figure 3) and to expand the range of parameter values for which the ratchet can work. Where it is operating, the 1D ratchet with parameters U, $s = \bar{s}$, and Ngives an overall rate of fitness loss that is very similar (within a factor of 2 where tested) to that of the exponentially distributed sites with U, $\bar{s}$,

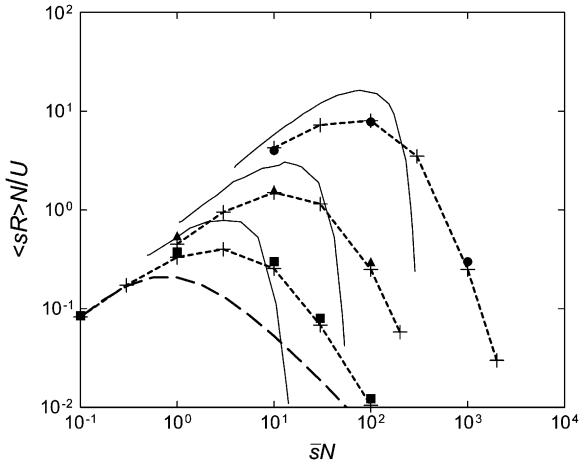

FIGURE 8.—Predicted scaled rate of fitness loss for an exponential distribution of *s*-values. Results are shown as a function of $\bar{s}N$ calculated from Equations 10–14; dotted lines are for $UN = 10^3$, 10^2, and 10 from top to bottom, and the lines were drawn between the calculated data points (crosses); solid data points are the simulated results from Table 2. The dashed line shows the expected result based on Equation 1 if all mutations accumulate independently and without background selection. The thin solid lines show the results for the 1D model with parameters *N*, *U*, and $s = \bar{s}$ using $UN = 10^3$, 10^2, and 10 from top to bottom.

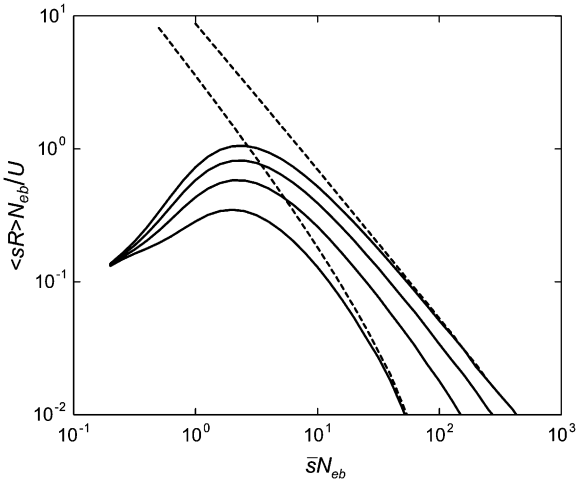

FIGURE 9.—Predicted scaled rate of fitness loss for an exponential distribution of *s*-values. Results are shown as a function of $\bar{s}N_{\rm eb}$ calculated from Equations 10, 11, 13, and 14. Solid lines from top to bottom are for $UN_{\rm eb} = 10^4$, 10^3, 10^2, and 10. The dotted lines are from Equation 15 for $UN_{\rm eb} = 10^4$ and 10.

and *N*. This may be surprising in light of the large variations in $N_{\rm eb}$ and the corresponding distinctions between the sites that are actually driven by the ratchet (Table 2).

Simulations have to be carried out with a given value of *N*, corresponding to the effective population size with no account taken of the background selection. The results in Table 2, also shown in Figure 8, confirm that background selection can be adequately accounted for by the effective population size $N_{\rm eb}$ through Equation 12. This $N_{\rm eb}$ is also the biologically relevant parameter as it is more directly coupled to the properties of the population than is the size *N*, in the presence of background selection. For instance, neutral diversity and fixation of weakly deleterious mutations depend on $N_{\rm eb}$ rather than *N* (CHARLESWORTH *et al.* 1993). Thus, in some cases it may be more interesting to consider the results in terms of $UN_{\rm eb}$ and $\bar{s}N_{\rm eb}$, as displayed in Figure 9. In contrast to the behavior in terms of UN and $\bar{s}N$ (Figure 8), the scaled fitness loss rate for the exponential distribution is much less sensitive to changes in $UN_{\rm eb}$ and it has its maximum at $\bar{s}N_{\rm eb} \approx 2$ irrespective of the value of $UN_{\rm eb}$. Also shown in Figure 9 is the result from the approximation in Equation 15, which works very well for $\bar{s}N_{\rm eb} \gg 4$ as expected. The value of *N* enters explicitly only in Equation 12, which shows the strength of the background selection; when $N_{\rm eb}$ is the known parameter, Equation 12 is not needed for the calculation of the ratchet rate.

Other assumptions: Distributions other than exponential can be described in the same way by inserting the appropriate distribution for averaging in Equations 10–13. The method can in principle be applied to any distribution of *s*-values, *e.g.*, the lognormal recently inferred for Drosophila (LOEWE and CHARLESWORTH 2006). The method is expected to work best for a broad distribution of effects where the exact location of the borders between categories is of less importance. It would not work well if all—or almost all—deleterious sites belong to category 1; the possibility of a slowly clicking ratchet in this category is not accounted for. We have tested the method also on a very narrow distribution of *s*-values, mimicking a 1D model with parameters *U*, *s*, *N*. It works surprisingly well also in this extreme (Table 3), except when most sites fall just inside the borderline to category 1. Even if all sites have the same *s*-value, the method can allocate different fractions of the sites to different categories. When $sN < 4$, all sites are in categories 2 or 3, $N_{\rm eb} = N$ holds, and the 1D model can be applied directly. When $sN > 4\exp(U/s)$, all sites are in category 1, $N_{\rm eb} = N\exp(-U/s)$, and the ratchet moves very slowly or not at all as assumed when applying the method. The interesting parameter region is $4 < sN < 4\exp(U/s)$, where the sites are divided between categories 1 and 2. The fraction allocated to category 1 can be calculated from Equation 7 by observing that the exponent simply gives the sum over the category 1 sites all with the same value for u/s. Thus, the fraction $(s/U)\ln(N/N_{\rm eb})$ of the sites are allocated to category 1 and the rest to category 2, while $N_{\rm eb} = 4/s$. Thus, in this region, the method would describe the 1D ratchet (parameters *U*, *s*, *N*) as a 1D ratchet with parameters ($U_2 = U - s\ln(sN/4)$, $s_2 = s$, $N_{\rm eb} = 4/s$). Computationally, there is of course no gain in this transformation, but as a test of the method it is informative.

TABLE 3

Average rate of fitness loss with a delta-function distribution of *s*-values

N	U	s	R^{1D}[a]	N_{eb}[b]	U_2[c]	s_2[c]	R_2^{1D}[d]
10^4	0.1	0.0006	0.060	6667	0.10	0.006	0.067
10^4	0.1	0.001	0.058	4000	0.099	0.001	0.062
10^4	0.1	0.003	0.039	1333	0.094	0.003	0.048
10^4	0.1	0.01	0.015	400	0.068	0.01	0.022
10^4	0.1	0.02	0.0031	200	0.022	0.02	0.0023

[a] Ratchet rate in the 1D Haigh model for the given values of N, U, and s.
[b] Effective population size calculated as $N_{eb} = 4/s$.
[c] Effective mutation rate and selection coefficient for the fraction of sites that are classified as category 2 as described in the text; the fraction of sites located in category 2 is U_2/U.
[d] Click rate in the category 2 sites calculated from a 1D Haigh model with parameters N_{eb}, U_2, and s_2. When s approaches 0.0243, R^{1D} of the Haigh model is $0.01U$ and all sites would be located in category 1 giving $U_2 = R_2^{1D} = 0$.

The choice of border between categories 1 and 2 was based on the behavior of the 1D and 2D ratchets. As can be seen in Table 2, it works well for the exponential distribution. However, it may not be the optimal choice under all circumstances. We have not systematically tested variations of this condition, but have for some cases (the last three entries in Table 2) tried shifting the border to $sN_{eb} > 5$, rather than 4. Such a shift results in an increase of the estimates of both U_2N_{eb} and s_2N_{eb}; the largest change occurs in the limit $\bar{s}N_{eb} \gg 1$, where s_2N_{eb} approaches 3, rather than 2.5, and U_2N_{eb} approaches $4U/\bar{s}$ rather than $3U/\bar{s}$. If U, $\bar{s}$, and N_{eb} are the given parameters, this increase occurs only in s_2 and U_2, while there will be an increase also in N_{eb} if U, $\bar{s}$, and N are the given parameters. As shown in Table 2, this leads to a slight increase in $\langle sR\rangle_2$ and a slight decrease in $\langle sR\rangle_3$ so that the total estimated fitness loss rate is only marginally affected (by a few percent), and there is no systematic improvement relative to the simulated rate.

It is also possible to use other methods of averaging the *s*-values in category 2. Using the harmonic mean or geometric mean to calculate s_2 in Equation 11 leads to a reduction of the estimate by at most 14 or 7%, respectively, in the limit $\bar{s}N_{eb} > 1$, and a much smaller reduction for smaller values of $\bar{s}N_{eb}$. By using a geometric average it could also be possible to adjust the border between groups 2 and 3 to values of sN_{eb} somewhat <1, making it possible to allow also for the weak interference that is expected in this parameter region. In view of the small differences and the uncertainty in all the assumed parameters, it does not seem worthwhile at this point to replace the simple arithmetic mean with some more complex averaging.

Thus, it is possible to reduce the general case with distributed *s*-values to a 1D calculation over the category 2 sites corresponding to Haigh's (1978) original model using the parameters U_2, s_2, and N_{eb}. To this should be added the near-independent accumulation of mutations in category 3. In some limits, the calculation can be very simple (Equation 15), and in others a simulation of the 1D model may be needed or the analytical approximations (Stephan *et al.* 1993; Gordo and Charlesworth 2000a,b; Stephan and Kim 2002) could be used. An approximate rate for the category 2 sites could also be read out of Figure 2, using U_2N_{eb} and s_2N_{eb} on the axes. It should be stressed that the size scaling holds also here such that $\langle sR\rangle N/U$ is invariant when N is varied at constant $\bar{s}N$ and UN, and also $\langle sR\rangle N_{eb}/U$ is invariant when N_{eb} is varied at constant $\bar{s}N_{eb}$ and UN_{eb}.

DISCUSSION AND CONCLUSIONS

Mutational interference shows up in some simple ways. First in the 1D model, by increasing the mutational target size, *i.e.*, increasing U, the ratchet rate increases more than directly proportionally to U as would have been expected in the model of independent sites (Equation 1). In the 2D model with two groups of mutations of different effect, we defined a window of interference (Figure 4). For many sets of parameters, this window is very small or absent, which means that the two ratchets work at too different a scale to have any effect on each other. The largest relative effects of one ratchet on the other occur when the ratchets would be stalled or nearly stalled if considered by themselves. In this case, the relative increase in click rate can be several orders of magnitude. The rate of fitness loss was affected in a similar but less dramatic way since the newly started ratchet would start from a very low level and therefore still has a low absolute rate.

The simulations were carried out with high reproducibility. The extent of the stochastic scatter in the 2D simulations can be seen in Figure 4, and the scatter was much smaller in 1D ($<1.5\%$ standard error). The simulation results were used to characterize the properties of the 1D and 2D ratchets with an emphasis on their limiting behavior. On the basis of the behavior of these idealized systems, we show how to describe more realistic situations where deleterious mutations have a range of

s-values. By necessity, this is much less exact but agrees well with simulations. However, there is not enough information known for any system that would warrant precise calculations; the main emphasis is on defining a method by which the behavior of the ratchet can easily be described as parameters or distributions change. The interference effects in the 1D and 2D models suggest an operational division of the deleterious mutations into three categories: (1) $4/N_{eb} < s < 1$, (2) $1/N_{eb} < s < 4/N_{eb}$, and (3) $0 < s < 1/N_{eb}$. One key consideration here is Equation 7, which defines N_{eb}, and therefore also these categories, from the distribution of *s*-values. The strongly deleterious sites in category 1 act mostly to determine the effective population size N_{eb}. The weakly deleterious ones in category 3 have little effect on the ratchet, but can contribute to fitness loss. Only sites that are in the narrow intermediate window (category 2) will be directly affected by the ratchet. It should be stressed that while the window of interference as seen in Figures 4 and 6 may be almost two orders of magnitude in sN-values, the sites in category 2 are defined much more narrowly within a factor of 4 in sN_{eb}. This difference is because a large part of the interference in Figures 4 and 6 comes from category 1 sites that themselves do not accumulate mutations. Also, the window of interference in terms of sN_{eb} is further compressed by the decrease in N_{eb} that will accompany an increasing s_2N in Figures 4 and 6. The slow clicking of the sites in category 1 has not been included because, when present, these sites will have their largest effect on the ratchet through background selection. This will not be a good approximation in the case that a large fraction of all deleterious sites are in category 1 just above the limit $sN_{eb} = 4$. Also, it is not impossible that rare clicks in this category could have a large effect on the immediate viability of the species and lead to mutational meltdown (Lynch *et al.* 1993). This would not show up in the simulations and calculations reported here, which deal only with the expected average rate of fitness loss without such threshold effects.

The distinction between the effective population sizes N and N_{eb} is crucial. N is the effective population size for freely recombining genomes where all mutations are segregating independently; this N is determined by the real population size and by effects from population structure and history. N_{eb} is the effective size for the same population when there is no recombination and all deleterious mutations are linked. Thus, it is reasonable to discuss the effects of linkage and Muller's ratchet in terms of the parameters U, s, and N to see what the loss of recombination in a given population would lead to (*cf.* Figures 3, 6, and 8). Also, the effects on the ratchet from variations in N may be more representative of the effects of changes in the real population size. In most natural populations, on the other hand, the effective population size is estimated from the neutral diversity. As neutral diversity is influenced by background selection (Charlesworth *et al.* 1993), it is usually N_{eb} of Equation 7 that is the known parameter. To discuss the fitness-loss rate in this case, it is therefore more reasonable to use the parameters U, s, and N_{eb} (Figure 9).

In the particular case of an exponential distribution of *s*-values with average $\bar{s}$, we find a very simple description that applies to a broad range of parameter values. The major effect of the distributed *s*-values is to expand the parameter region where the ratchet can be expected to operate. In this case there is no sharp dividing line in parameter space where the ratchet can be said to have stopped. This is not unexpected since even for large $\bar{s}N$ there will always be weakly deleterious mutations possible (Butcher 1995). More surprising, perhaps, is the finding that the overall rate of fitness loss is very similar (within approximately half) to that expected from a 1D Haigh model where all sites have the selection $\bar{s}$ and parameters (U, $\bar{s}$, N); this holds in the parameter region where the 1D ratchet can operate and for the parameter values tested (Figure 8). This near agreement is based on the population size N being the same in the two models.

In a recent article, Loewe (2006) discusses the expected extinction time of the human mitochondrial line due to Muller's ratchet. To estimate the threat of extinction, both analytical approximations and 1D simulations were used to show that the threat of extinction due to Muller's ratchet cannot be neglected over 20 MY evolutionary time. The U-shaped extinction time *vs.* selection discussed by him corresponds roughly to the inverse of the fitness-loss curves in Figures 3, 6, and 8 above. However, Loewe's calculations also include an actual extinction step that occurs when so much fitness has been lost that the population cannot be expected to reproduce itself, leading to mutational meltdown (Lynch and Gabriel 1990; Lynch *et al.* 1993). Loewe (2006) also suggests focusing on the most critical range of selection coefficients, those that will contribute most strongly to the fitness degeneration; these correspond roughly to our category 2 sites, but with borderlines defined somewhat differently.

Expected fitness degeneration in bacteria: Drake (1991) has identified mutation rates in different microorganisms spanning a wide range of genome sizes and found a genomic rate that is virtually invariant at $U = 0.003$ per generation. While this number is not universally accepted, it is a reasonable starting point for discussion. As perhaps half of all mutations are expected to be deleterious to some degree, $U/2$ could be a rough estimate for the deleterious mutation rate. The average selection coefficient has also been identified in a few cases. In *Escherichia coli*, Kibota and Lynch (1996) found an average $\bar{s} = 0.012$ and genomic mutation rate $U = 0.00017$. Similarly, in Salmonella, $\bar{s} = 0.04$ and $U = 0.0004$ have been estimated (Maisnier-Patin *et al.* 2005). These measured *s*-values would correspond to the weighted arithmetic averages over all possible deleterious or neutral mutations in the genome, except

those that are lethal. If all mutations have the same *s*-value and $\bar{s}$ and U are in this range, the ratchet would be way outside its range of operation (consider the diagonal at $sN/UN = 100$ in Figure 2). On the other hand, the deleterious effects are more likely to be distributed over a wide range of *s*-values between 0 and 1. If, for the sake of discussion, we assume an exponential distribution where $U = 0.0003$, $\bar{s} = 0.01$, and use the estimated effective population size $N_{eb} = 10^8$ (Hartl *et al.* 1994) one finds $N_{eb}/N = 0.7$ from Equation 12. Thus, the measured values for mutation and average selection—assuming an exponential distribution—are just in a region where background selection can be expected to contribute significantly to the effective population size. With these numbers, one finds $U_2N_{eb} = 0.09$ and $s_2N_{eb} = 2.5$, which give an estimated fitness loss rate that is vanishingly small, $\langle sR \rangle \approx 10^{-19}$, also with the distributed *s*-values. As the 1D and exponential distributions are two extremes of all possible distributions, it is unlikely that any distribution of intermediate shape could allow a significant clicking with these parameter values. The measured U and $\bar{s}$-values actually include neutral mutations. If these form a significant fraction, f_0, of all mutations and form a group outside of the exponential distribution, then the exponential distribution would have the average $\bar{s} = 0.01/(1 - f_0)$; this leads to a decrease in U_2N_{eb} by a factor $(1 - f_0)^2$ while s_2N_{eb} remains unchanged. The result would be a further reduction in the estimated fitness-loss rate.

Although Muller's ratchet has not been thought to operate in *E. coli* or Salmonella, except under very special circumstances (Andersson and Hughes 1996), the calculations show that with the estimated values for U and *s*, Muller's ratchet cannot operate in the wild type regardless of the population size. In fact, with similar values of U and *s*, most free-living microbes are not expected to be affected by the ratchet. Prime candidates for Muller's ratchet are intracellular symbionts and parasites, which rarely have the opportunity for recombination (Moran 1996; Rispe and Moran 2000). As an extreme example of an intracellular symbiont, the degeneration of mitochondrial genomes has been suggested to be a consequence of Muller's ratchet (Lynch 1996; Bergstrom and Pritchard 1998; Lynch and Blanchard 1998; Loewe 2006). The effects on the ratchet from the particular population structure and dynamics governing symbionts have been discussed in a separate article (Pettersson and Berg 2007), using the obligatory endosymbiont Buchnera in aphids as an example. Buchnera is transmitted maternally and goes through cycles of growth and bottlenecks coupled to the aphid generations. Each vertical line of Buchnera is a clone of small effective population size that is determined primarily by the size of the transmission bottleneck. As a consequence, deleterious mutations that affect only the well-being of Buchnera are expected to accumulate. On the other hand, Buchnera is an obligatory symbiont and mutations that severely affect its fitness are also likely to affect the host detrimentally. The aphids have a large effective population size and host-level selection is therefore expected to be significant. That is, the dynamics of mutation appearance are determined on the symbiont level while selection is mostly on the host level. The ensuing nested-population dynamics can be described essentially on the host level if the mutation rate and the effective population size of Buchnera are counted per host generation. Assuming that all deleterious mutations have the same effect, *s*, on the host, it was estimated (Pettersson and Berg 2007) that Muller's ratchet could not operate in this system if $s > 10^{-4}$ or so. The numbers used correspond to the parameter values $N_{eb} = 10^5$ and $U = 5 \times 10^{-4}$ expressed per host generation. The criterion, Equation 4, would give $sN_{eb} > 30$ as the limit where the 1D ratchet stops ($sR^{1D} < 1.5 \times 10^{-9}$). For smaller U and/or larger *s*, the 1D ratchet will effectively have stopped. For this value of UN_{eb} ($= 50$), $s = 10^{-4}$ ($sN_{eb} = 10$) would give a close-to-maximal fitness-loss rate (Equation 6) with $sR^{1D} = 10^{-8}$ per host generation. If instead the deleterious effects have an exponential distribution with average $\bar{s} = 10^{-4}$, Equations 13 and 14 predict an even smaller fitness loss rate of $\langle sR \rangle = 10^{-9}$. For larger average *s*-values, where the 1D model would have stopped, *e.g.*, $\bar{s} = 10^{-3}$ or 10^{-2}, Equations 13 and 14 predict $\langle sR \rangle = 6 \times 10^{-11}$ or 3×10^{-12}, respectively. For an exponential distribution of *s*-values, there is—in contrast to the 1D model—no sharp dividing line in parameter space where the ratchet can be considered as stopped. With a higher symbiont mutation rate ($U = 10^{-3}$ per host generation), the estimated fitness-loss rates would be $\langle sR \rangle = 3 \times 10^{-9}$, 2×10^{-10}, and 6×10^{-12} for average $\bar{s} = 10^{-4}$, 10^{-3}, and 10^{-2}, respectively. Such slow rates are likely to be counteracted by back mutations or compensatory mutations. It seems unlikely that the average deleterious effect in Buchnera would be much smaller than that measured in *E. coli*, on the order of 10^{-2} (including neutral mutations). Thus, the conclusion (Pettersson and Berg 2007) that the ratchet at present would operate very slowly in this system holds also if the deleterious effects have an exponential distribution.

Fitness degeneration of the Y chromosome: Gordo and Charlesworth (2000a) discuss the degeneration of the Y chromosome in Drosophila using the assumptions $N_{eb} = 5 \times 10^5$, $U = 0.04$, and $\bar{s} = 0.01$. Considered as a 1D ratchet with values $UN = UN_{eb} = 2 \times 10^4$ and $sN = \bar{s}N_{eb} = 5 \times 10^3$, this is clearly outside the window of operation (Figure 2), with an estimated rate of fitness loss $sR = 3 \times 10^{-28}$ (Gordo and Charlesworth 2000a). But it is also in a parameter region where small changes in sN or UN could have huge effects on the ratchet; an increase in U from 0.04 to 0.06 increases the expected rate by ~20 orders of magnitude (Gordo and Charlesworth 2000a). If instead it is assumed that *s*-values have an exponential distribution with average

$\bar{s} = 0.01$, the ratchet can be expected to operate on the subset of mutations that belong in category 2. Then, $\bar{s}N_{eb} \gg 4$ and $U/\bar{s} = 4$ hold, which gives $s_2 N_{eb} \approx 2.5$, $U_2 N_{eb} \approx 12$, and $N_{eb}/N = 0.88$. Thus, the requirements for the approximations behind Equation 15 hold and the total rate of fitness loss is $\langle sR \rangle \approx 4.6 \times 10^{-11}$. This would correspond to the fixation of a deleterious mutation of average effect once every 2×10^8 generations. This is still an exceedingly slow rate, but much faster than that expected from the 1D model. However, in contrast to the 1D case, a change in U from 0.04 to 0.06 would increase the ratchet rate by less than a factor of 2 (Equation 15) in the case of an exponential distribution of s-values. Thus, with the distributed effects, small changes in the parameters (U, $\bar{s}$, N_{eb}) will not have large effects on the ratchet, and with the parameters assumed, the ratchet will remain stalled. However, this discussion is based on the assumption that the given effective population size ($N_{eb} = 5 \times 10^5$) already includes the effects (if any) from the background selection among the distributed sites. If this is not the case, the assumed effective population size would correspond to N. With $N = 5 \times 10^5$, $\bar{s} = 0.01$, and $U = 0.04$ one finds $\langle sR \rangle = 2 \times 10^{-6}$ (Equations 12–14) for the exponentially distributed sites. In this case, background selection would decrease the effective population size to a point where the ratchet rate is significant.

Another kind of mutational interference that has not been addressed in these calculations is epistasis, where two mutations that individually are counterselected by s_1 and s_2 together are counterselected by more (synergistic) or less (antagonistic) than $s_1 + s_2$. It has been suggested that synergistic epistasis could stop the ratchet by progressively increasing the effective counterselection for new mutations when some have already been accumulated (Kondrashov 1994). However, it seems that synergistic epistasis is of little help to stop the ratchet if s-values have a distribution that includes those of small effect (Butcher 1995). Of even more consequence, perhaps, is the observation that deleterious mutations can be buffered (Maisnier-Patin *et al.* 2005) such that the effect of a new deleterious mutation is weaker when others are already present. Clearly, this kind of antagonistic epistasis could significantly speed up mutation accumulation. On the other hand, the actual fitness loss would be buffered and could perhaps be less severe.

We thank Mats Pettersson for numerous discussions. This work was supported by The Swedish Research Council.

LITERATURE CITED

Andersson, D. I., and D. Hughes, 1996 Muller's ratchet decreases fitness of a DNA-based microbe. Proc. Natl. Acad. Sci. USA **93:** 906–907.

Barton, N. H., and B. Charlesworth, 1998 Why sex and recombination? Science **281:** 1986–1990.

Bergstrom, C. T., and J. Pritchard, 1998 Germline bottlenecks and the evolutionary maintenance of the mitochondrial genome. Genetics **149:** 2135–2146.

Butcher, D., 1995 Muller's ratchet, epistasis and mutation effects. Genetics **141:** 431–437.

Charlesworth, B., 1994 The effect of background selection against deleterious mutations on weakly selected, linked variants. Genet. Res. **63:** 213–227.

Charlesworth, B., and D. Charlesworth, 1997 Rapid fixation of deleterious alleles can be caused by Muller's ratchet. Genet. Res. **70:** 63–73.

Charlesworth, B., M. T. Morgan and D. Charlesworth, 1993 The effect of deleterious mutations on neutral molecular variation. Genetics **134:** 1289–1303.

Dolgin, E. S., and B. Charlesworth, 2006 The fate of transposable elements in asexual populations. Genetics **174:** 817–827.

Drake, J. W., 1991 A constant rate of spontaneous mutation in DNA-based microbes. Proc. Natl. Acad. Sci. USA **88:** 7160–7164.

Ewens, W. J., 1979 *Mathematical Population Genetics.* Springer-Verlag, Berlin.

Felsenstein, J., 1974 The evolutionary advantage of recombination. Genetics **78:** 737–756.

Gessler, D. D. G., and S. Xu, 1999 On the evolution of recombination and meiosis. Genet. Res. **73:** 119–131.

Gordo, I., and B. Charlesworth, 2000a The degeneration of asexual haploid populations and the speed of Muller's ratchet. Genetics **154:** 1379–1387.

Gordo, I., and B. Charlesworth, 2000b On the speed of Muller's ratchet. Genetics **156:** 2137–2140.

Gordo, I., and B. Charlesworth, 2001 The speed of Muller's ratchet with background selection, and the degeneration of Y chromosomes. Genet. Res. **78:** 149–161.

Haigh, J., 1978 The accumulation of deleterious genes in a population – Muller's ratchet. Theor. Popul. Biol. **14:** 251–267.

Hartl, D. L., E. N. Moriyama and S. A. Sawyer, 1994 Selection intensity for codon bias. Genetics **138:** 227–234.

Hurst, L. D., and J. R. Peck, 1996 Recent advances in understanding of the evolution and maintenance of sex. Trends Ecol. Evol. **11:** 46–52.

Keightly, P. D., and A. Eyre-Walker, 2000 Deleterious mutations and the evolution of sex. Science **290:** 331–333.

Kibota, T. T., and M. Lynch, 1996 Estimate of the genomic mutation rate deleterious to overall fitness in *E. coli.* Nature **381:** 694–696.

Kimura, M., 1962 On the probability of fixation of mutant genes in a population. Genetics **47:** 713–717.

Kimura, M., 1964 Diffusion models in population genetics. J. Appl. Probab. **1:** 197–232.

Kondrashov, A. S., 1994 Muller's ratchet under epistatic selection. Genetics **136:** 1469–1473.

Loewe, L., 2006 Quantifying the genomic decay paradox due to Muller's ratchet in human mitochondrial DNA. Genet. Res. **87:** 133–159.

Loewe, L., and B. Charlesworth, 2006 Inferring the distribution of mutational effects on fitness in *Drosophila.* Biol. Lett. **2:** 426–430.

Lynch, M., 1996 Mutation accumulation in transfer RNAs: molecular evidence for Muller's ratchet in mitochondrial genomes. Mol. Biol. Evol. **13:** 209–220.

Lynch, M., and L. Blanchard, 1998 Deleterious mutation accumulation in organelle genomes. Genetica **102/103:** 29–39.

Lynch, M., and W. Gabriel, 1990 Mutation load and the survival of small populations. Evolution **44:** 1725–1737.

Lynch, M., R. Bürger, D. Butcher and W. Gabriel, 1993 The mutational meltdown in asexual populations. J. Hered. **84:** 339–344.

Maisnier-Patin, S., J. R. Roth, Å. Fredriksson, T. Nyström, O. G. Berg *et al.*, 2005 Genomic buffering mitigates the effects of deleterious mutations in bacteria. Nat. Genet. **37:** 1376–1379.

Maynard Smith, J., 1978 *The Evolution of Sex.* Cambridge University Press, Cambridge, UK.

McVean, G., and B. Charlesworth, 1999 A population genetic model for the evolution of synonymous codon usage: patterns and predictions. Genet. Res. **74:** 145–158.

McVean, G., and B. Charlesworth, 2000 The effects of Hill–Robertson interference between weakly selected mutations on patterns of molecular evolution and variation. Genetics **155:** 929–944.

Moran, N. A., 1996 Accelerated evolution and Muller's ratchet in endosymbiont bacteria. Proc. Natl. Acad. Sci. USA **93:** 2873–2878.

Moran, P. A. P., 1958 Random processes in genetics. Proc. Camb. Philos. Soc. **54:** 60–71.

Muller, H. J., 1964 The relation of recombination to mutational advance. Mutat. Res. **1:** 2–9.

Pettersson, M. E., and O. G. Berg, 2007 Muller's ratchet in symbionts populations. Genetica **130:** 199–211.

Rice, W. R., 1994 Degeneration of a nonrecombining chromosome. Science **263:** 230–232.

Rispe, C., and N. A. Moran, 2000 Accumulation of deleterious mutations in endosymbionts: Muller's ratchet with two levels of selection. Am. Nat. **156:** 425–441.

Stephan, W., and Y. Kim, 2002 Recent application of diffusion theory to population genetics, pp. 72–93 in *Modern Developments in Theoretical Population Genetics*, edited by M. Slatkin and M. Veuille. Oxford University Press, Oxford.

Stephan, W., L. Chao and J. G. Smale, 1993 The advance of Muller's ratchet in a haploid asexual population: approximate solutions based on diffusion theory. Genet. Res. **61:** 225–231.

Stephan, W., B. Charlesworth and G. McVean, 1999 The effect of background selection at a single locus on weakly selected, partially linked variants. Genet. Res. **73:** 133–146.

Waterson, G. A., 1975 On the number of segregating sites in general models without recombination. Theor. Popul. Biol. **7:** 256–276.

Communicating editor: J. B. Walsh